



**AIAA 2001-3082**

**SPACE SHUTTLE UPGRADE  
LIQUID OXYGEN TANK  
THERMAL  
STRATIFICATION**

Gokturk Tunc  
Howard Wagner  
Yildiz Bayazitoglu

Rice University  
Houston, Texas

**35<sup>th</sup> AIAA Thermophysics  
Conference  
11-14 June 2001/Anaheim, CA**

# SPACE SHUTTLE UPGRADE LIQUID OXYGEN TANK THERMAL STRATIFICATION

Gokturk Tunc<sup>+</sup>, Howard Wagner<sup>+</sup>, and Yildiz Bayazitoglu<sup>‡</sup>

Mechanical Engineering and Materials Science Department

Rice University

6100 Main St., MS 321

Houston, Texas 77005, USA

## Abstract

In 1997, NASA initiated a study of a liquid oxygen and ethanol orbital maneuvering and reaction control system for space shuttle upgrades as well as other reusable launch vehicle applications. The pressure-fed system uses sub-cooled liquid oxygen at 2413.2 KPa (350 psia) stored passively using insulation. Thermal stratification builds up while the space shuttle is docked at the international space station. The venting from the space shuttle's liquid oxygen tank is not desired during this 96-hr time period. Once the shuttle undocks from the space station there could be a pressure collapse in the liquid oxygen tank caused by fluid mixing due to the thruster firings. The thermal stratification and resulting pressure rise in the tank were examined by a computational fluid dynamic model. Since the heat transfer from the pressurant gas to the liquid will result in a decrease in tank pressure the final pressure after the 96 hours will be significantly less when the tank is pressurized with ambient temperature helium. Therefore, using helium at ambient temperature to pressurize the tank is preferred to pressurizing the tank with helium at the liquid oxygen temperature. The higher helium temperature will also result in less mass of helium to pressurize the tank.

## Nomenclature

$C_p$ : Specific heat, J/Kg-K  
 $F$ : Body forces, N  
 $g$ : Gravity vector, 9.81 m/s<sup>2</sup>  
 $h$ : Enthalpy, J/Kg  
 $k$ : Thermal conductivity, W/m-K  
 $m$ : Mass, Kg  
 $M$ : Molecular weight, Kg/Kmol  
 $P$ : Pressure, N/m<sup>2</sup>  
 $P_{op}$ : Operating pressure, N/m<sup>2</sup>  
 $P$ : Pressure update, N/m<sup>2</sup>

$\bar{R}$ : Universal gas constant, 8.314 KJ/Kmol-K

$u_j$ : Velocity component, m/s

$S_e$ : Source term for continuity equation, 1/s

$S_h$ : Source term for energy equation, W/m<sup>3</sup>

$t$ : Time, s

$T$ : Absolute temperature, K

$x_j$ : Spatial domain variable, m

## Greek Letters

$\alpha$ : Mass fraction

$\epsilon$ : Volume fraction

$\gamma$ : Specific heat ratio

$\mu$ : Dynamic viscosity, Kg/m-s

$\rho$ : Density, Kg/m<sup>3</sup>

$\upsilon$ : Specific volume, m<sup>3</sup>/Kg

## Introduction

NASA has initiated an effort to look at a liquid oxygen and ethanol orbital maneuvering (OMS) and reaction control system (RCS) for space shuttle upgrades. Numerous trade studies<sup>1-4</sup> conducted from 1980 to 1996 have shown that liquid oxygen and ethanol are the two most appropriate fluids for a pressure-fed system. Liquid oxygen and ethanol are clean-burning, high-density propellants that provide a high degree of commonality with other spacecraft subsystems including life support, main propulsion, power, and thermal control. The use of liquid oxygen will reduce the number of different fluids and propellants used on the space shuttle. These propellants will support a variety of reusable launch vehicles (RLV) for future human exploration. Historically most vehicles have used earth-storable propellants for the OMS/RCS, however liquid oxygen combined with passive insulation is suitable for reusable vehicles with up to 30 day on-orbit stay

<sup>+</sup> Graduate student

<sup>‡</sup> Professor

time; and for longer duration, over years, cryo-coolers can be used to eliminate the boil-off. Oxygen can also be tapped off the tanks for life support or fuel cell reactants. The key to this pressure-fed system is the use of sub-cooled liquid oxygen at 2413.2 KPa (350 psia). In this approach, there is 44.4 K (80 R) of sub-cooling, which means that boil-off will not occur until the temperature has risen 44.4 K. The sub-cooling results naturally from loading propellants at 90.6 K (163 R), which is the saturation temperature at 101.325 KPa (14.7 psia), and then pressurizing to 2413.2 KPa (350 psia) on the launch pad. Thermal insulation and conditioning techniques are then used to limit the liquid oxygen temperature to a 102.8 K (185 R) maximum to maintain sub-cooling. Another important factor to consider is the wide melting point to boiling point temperature range of ethanol, 159.4 K to 422.2 K (-173 F to +300 F), which can provide heat to gasify the liquid oxygen or provide a good coolant.

The rationale for using non-toxic propellants are to improve safety, reduce cost, increase the flight rates, and improve mission capability. The non-toxic OMS/RCS design addresses each of these goals. It reduces ground and flight safety hazards with the elimination of the current toxic and corrosive propellants. The cost savings for shuttle ground operations are estimated to be over \$26 million for 8 flights per year, and the savings will increase with increasing flight rates. Using non-toxic propellants reduces the serial processing time by 75% during ground turnaround. This will also support dramatically higher flight rates. The payload capability is significantly increased by 1134.0 Kg to 1496.9 Kg (2500 to 3300 lbm) due to increased OMS engine performance. By interconnecting the aft and forward tanks and by adding redundant verniers, the non-toxic OMS/RCS improves space station reboost capability by up to 20 nautical miles. The redundant verniers are added by using dual thrust RCS engines, which also improves mission success reliability.

### Thermal Stratification

The issue being addressed in this paper is the extent of the thermal stratification that could build up while the space shuttle is docked at the international space station. During this 96-hr time period, it is desired to have no venting from the space shuttle's liquid oxygen tanks. The thermal stratification and resulting pressure rise in the tank during this time was examined by performing a computational fluid

dynamic assessment of the liquid oxygen tank. When the shuttle undocks from the space station there could be a pressure collapse in the liquid oxygen tank caused by fluid mixing, which results from the thruster firings.

The liquid oxygen tank was modeled using the computational fluid dynamic software FLUENT, created by Fluent, Inc. Running the full 3D model requires extensive computer memory and time. Therefore, an axisymmetric 2D model of the tank was created that gives the opportunity to run different cases in a reasonable amount of time. The Volume of Fluid (VOF) technique is used by FLUENT to model multiphase problems. The fluids share a single set of momentum equations. For each additional phase a volume fraction is defined. The volume fraction of each phase is tracked through the computational domain. Surface tension effects were also included.

Mass transfer between the liquid and gaseous oxygen was not included in the analyses. Previous studies in microgravity liquid acquisition<sup>5-17</sup> show that when the tank is pressurized with gaseous oxygen the vapor at the interface condenses onto the liquid oxygen. The increase in the heat transfer decreases the surface tension. However, when the tank is pressurized using helium no mass transfer occurs at the interface. Since there is no convection the mass transfer at the liquid/vapor interface is limited by the diffusion of oxygen vapor through the gaseous helium, which proceeds very slowly because of the equality of their temperatures. Therefore, mass transfer can safely be neglected in the simulations.

### Analysis

The following set of equations is solved in the VOF model. The compressible version of the ideal gas law is used to calculate the gas density.

Equation of state

$$\rho = \frac{(P_{op} + P')M}{RT} \quad (1)$$

where  $P_{op}$  is the operating pressure and  $P'$  is the pressure update. The operating pressure is a constant reference pressure and the pressure update is the time varying pressure. The density variation is accommodated by the time varying component of the pressure.

Continuity for the volume fraction of the vapor phase is given by

$$\frac{\partial \varepsilon}{\partial t} + u_j \frac{\partial \varepsilon}{\partial x_j} = S_\varepsilon \quad (2)$$

Momentum equation

$$\frac{\partial}{\partial t} (\rho u_j) + \frac{\partial}{\partial x_i} \rho u_i u_j = -\frac{\partial P}{\partial x_j} + \frac{\partial}{\partial x_j} \mu \left( \frac{\partial u_i}{\partial x_j} + \frac{\partial u_j}{\partial x_i} \right) + \rho g_j + F_j \quad (3)$$

Energy equation

$$\frac{\partial}{\partial t} (\rho h) + \frac{\partial}{\partial x_i} \rho u_i h = \frac{\partial}{\partial x_i} \left( k \frac{\partial T}{\partial x_i} \right) - \varepsilon_i S_h \quad (4)$$

FLUENT uses the Semi-Implicit Method for Pressure Linked Equations (SIMPLE) to solve the above system of equations<sup>18</sup>. The convergence criterion for all variables except enthalpy is  $10^{-3}$ . When solving the energy equation a  $10^{-6}$  convergence was satisfied. In order to ensure the stability and damp out nonlinearities, small values of underrelaxation were applied to update the parameters. Larger values were needed for faster convergence.

Nine different cases were evaluated to determine the effects of the different parameters on the final tank pressure. The tank is loaded with liquid oxygen at different initial conditions as saturated liquid at 241.3 KPa (35 psi) and 101.325 KPa (14.7 psi) with 85% and 65% fill levels ('fill level' indicates the volume occupied by the liquid phase). These two fill levels were selected as being representative of the liquid quantities that would be remaining in the liquid oxygen tank at the time that the space shuttle docks to the space station. The tank is then pressurized to 2413.2 KPa (350 psi) using helium at two different temperatures, ambient temperature and the temperature of the liquid oxygen. The effect of boundary heating is also evaluated for various heat flux values. In the following section a sample calculation is given for Case 1.

#### Evaluation of the initial conditions for Case 1

In this case the liquid and vapor oxygen are starting at the saturation conditions at a pressure of 241.3 KPa (35 psi). Helium is then introduced into the tank to increase the pressure to 2413.2 KPa (350 psia).

The volume occupied by the liquid oxygen is 85% of the total tank volume and will be referred to as "85% fill level". Boundary heat flux at the wall is 6.31 W/m<sup>2</sup> (2 BTU/hr-ft<sup>2</sup>). The properties of the liquid and vapor phases after pressurization are calculated. The liquid phase is pure oxygen whereas the vapor phase is a mixture of oxygen and helium. The fluid properties are obtained from the computer code released by the National Institute of Standards and Technology (NIST)<sup>19</sup>. The pressurization process is assumed to be fast enough that we can make an isentropic compression assumption. The following relation is used to obtain the temperature of the vapor oxygen after the pressurization process:

$$\frac{T_2}{T_1} = \left( \frac{P_2}{P_1} \right)^{\frac{\gamma-1}{\gamma}} = \left( \frac{350}{35} \right)^{\frac{0.48}{1.48}} = 2.110203 \quad (5)$$

where  $T_1$  is the saturation temperature of vapor oxygen at 241.3 KPa (35 psi). Then  $T_2 = 209.733$  K (377.5 R). The volume reduction of the vapor oxygen due to compression can be obtained as

$$\frac{v_2}{v_1} = \left( \frac{P_1}{P_2} \right)^{1/\gamma} = \left( \frac{35}{350} \right)^{1/1.48} = 0.2102 \quad (6)$$

The ratio of the vapor oxygen volume before and after the pressurization is calculated using the conservation of mass principal.

$$m_{O_2} = \frac{V_1}{v_1} = \frac{V_2}{v_2} \Rightarrow \frac{v_2}{v_1} = \frac{V_2}{V_1} = 0.2102 \quad (7)$$

This shows that after He is pumped into the tank 21% of the initial vapor volume is occupied by vapor oxygen and 79% is occupied by helium. To calculate the mixture properties the mass fraction of the gases must be known. First the properties of both gases will be obtained and then using the densities the mass fraction will be computed. After pressurization vapor oxygen has the following properties

$$\begin{aligned} T &= 209.73 \text{ K} & P &= 2413.18 \text{ KPa} \\ \rho &= 47.24 \text{ Kg/m}^3 & \mu &= 15.85e-6 \text{ Kg/m-s} \\ C_p &= 1017.754 \text{ J/Kg-K} & k &= 0.02071598 \text{ W/m-K} \end{aligned}$$

Helium properties are as follows:

$$\begin{aligned} T &= 209.73 \text{ K} & P &= 2413.18 \text{ KPa} \\ \rho &= 5.45 \text{ Kg/m}^3 & \mu &= 15.79e-6 \text{ Kg/m-s} \\ C_p &= 5193.8 \text{ J/Kg-K} & k &= 0.123716 \text{ W/m-K} \end{aligned}$$

The mass fraction of helium is given by

$$\alpha_{He} = \frac{m_{He}}{m_{O_2} + m_{He}} = 0.3 \quad (8)$$

Finally, any property P is calculated based on mass averages.

$$P = \alpha_{O_2} P_{O_2} + \alpha_{He} P_{He} \quad (9)$$

The only information that is needed to start the simulation is the liquid oxygen properties, which are the saturation properties at 241.3 KPa (35 psi). The simulation starts after the pressurization period. Therefore, the property values mentioned above are the initial conditions. The initial conditions for all of the simulations are given in Table 1. A  $1 \times 10^{-5}$  g gravity vector is applied for all the simulations so that the initial position of the liquid is known.

The axisymmetric model, Figure 1, is run to obtain the thermal conditions at the end of the four-day period. Then the data is used to generate a 3D model, Figure 2, by using symmetry. Then the gravity vector is applied in the opposite direction with a magnitude of  $1e-2$  g, which is believed to be the worst case as far as fluid mixing and thus pressure collapse is concerned. The 3D runs continued until the pressure recovers itself.

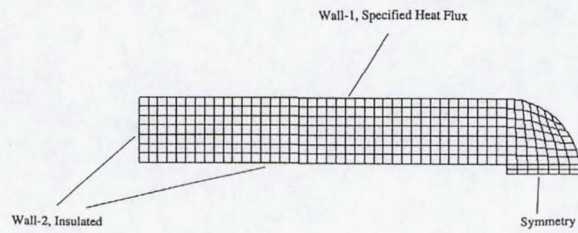


Figure 1. 2D-axisymmetric geometry of the tank

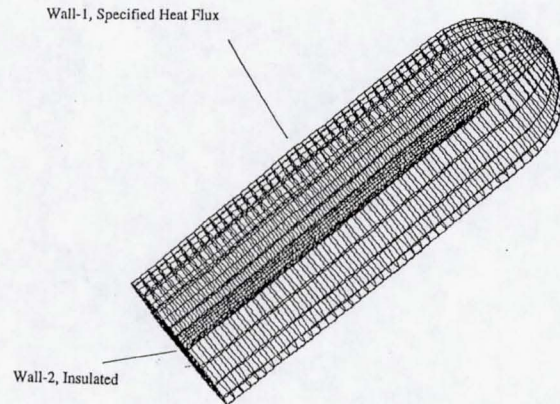


Figure 2. 3D tank geometry with the boundary conditions

Case	1	2	3	4	5	6	7	8	9*
Fill Level, %	85	65	85	85	65	85	85	85	85
Initial Tank Pressure KPa	241.3	241.32	101.325	101.325	101.325	101.325	101.325	101.325	101.325
Initial Tank Temperature, K	99.95	99.95	99.39	99.39	99.39	99.39	99.39	99.39	99.39
Liquid Temp. after pressurization, K	99.95	99.95	99.39	99.39	99.39	99.39	99.39	99.39	99.39
Mass fraction of Helium	0.3	0.3	0.488	0.711	0.711	0.488	0.488	0.711	0.711
Gas Temp. after pressurization, K	209.7	209.73	237.607	132.8	132.8	237.61	237.61	132.8	132.8
Boundary Flux, W/m <sup>2</sup>	6.31	6.31	6.31	6.31	67.8	3.15	67.8	67.8	67.8

Table 1. Initial and boundary conditions for different cases

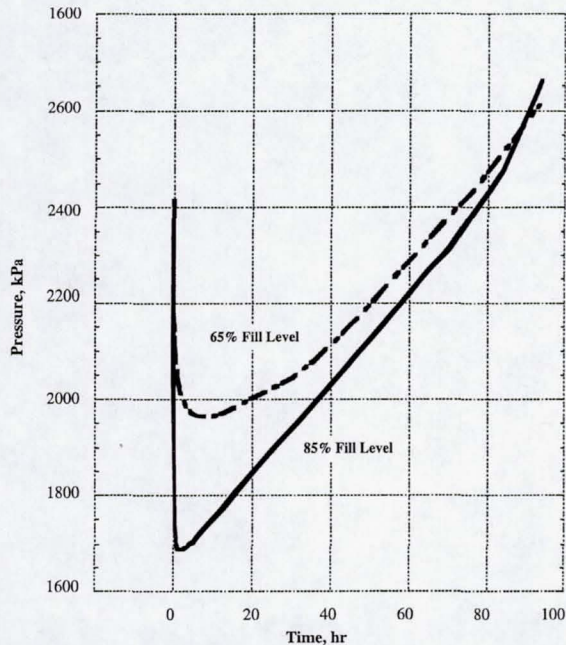
\*The thermodynamic vent system (TVS) is operated continuously to maintain a constant temperature of 80.6 K at the centerline of the tank.

**Results**

Figure 3 shows the effect that the liquid fill level has on the tank pressure when the tank is loaded with

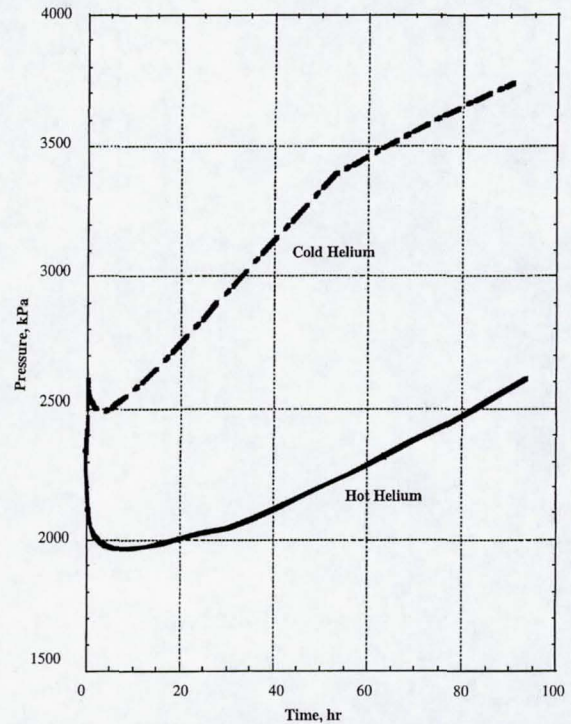
liquid oxygen saturated at 241.3 KPa (35 psi) pressure. In both cases the tank was pressurized with ambient temperature helium (hot helium case). The energy from the vapor region is initially transferred

to the liquid region until the liquid and vapor at the interface reach an equilibrium temperature. The pressure in the tank decreases during this period. After an equilibrium temperature is reached the environmental heat input causes the ullage temperature and pressure to increase.



**Figure 3.** Effect of liquid fill level on pressure rise when the tank is loaded with liquid oxygen saturated at 241.3 KPa (35 psi) pressure.

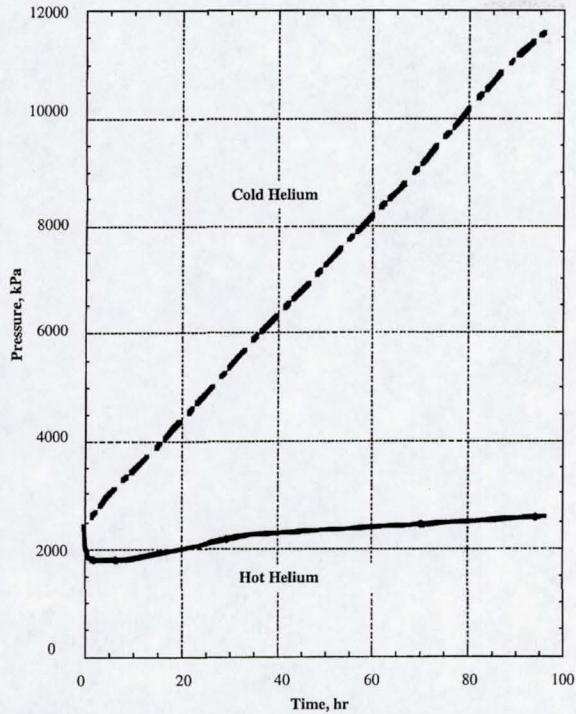
Figure 4 shows the effect of helium temperature on the pressure change when the liquid fill level is at 65%. The hot helium case is when the tank was pressurized with ambient temperature helium. The cold helium case is when the tank was pressurized with helium at the liquid oxygen temperature. In the hot helium case the energy from the vapor region is initially transferred to the liquid region until the liquid and vapor at the interface reach an equilibrium temperature. The pressure in the tank decreases during this period. After an equilibrium temperature is reached the environmental heat input causes the ullage temperature and pressure to increase. In the cold helium case the ullage pressure immediately starts to increase since the liquid and vapor are already at an equilibrium temperature.



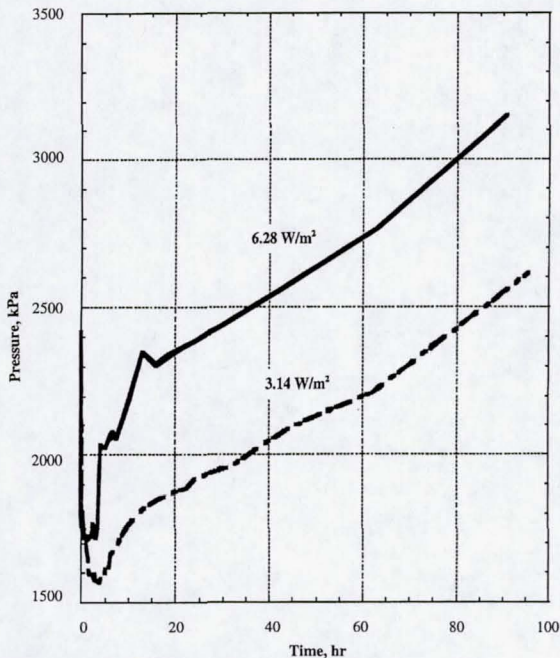
**Figure 4.** Effect of helium temperature on the pressure change when the liquid fill level is at 65%.

Figure 5 shows the effect of the helium temperature on the pressure change when the liquid fill level is at 85% and the tank has suffered a failure in the insulation system. The heat flux has increased to  $67.8 \text{ W/m}^2$  ( $21.5 \text{ BTU/hr-ft}^2$ ) to simulate the loss of the thermal insulation system.

Figure 6 shows the effect of varying the heat flux on the pressure in the tank at a liquid fill level of 85%. In both cases the tank was pressurized with ambient temperature helium. Two different environmental heat leak values were investigated,  $6.31 \text{ W/m}^2$  ( $2 \text{ BTU/hr-ft}^2$ ) and  $3.15 \text{ W/m}^2$  ( $1 \text{ BTU/hr-ft}^2$ ). As expected the pressure recovery occurs faster with a larger heat input.



**Figure 5.** Effect of helium temperature on the pressure change when the liquid fill level is at 85% and the tank has suffered a failure in the insulation system.



**Figure 6.** Effect of varying the heat flux on the pressure in the tank at a liquid fill level of 85%.

Figure 7 shows the ability of the thermodynamic vent system (TVS) to control the tank pressure following

the loss of the insulation system. In both cases the tank was pressurized with helium at the liquid oxygen temperature. In the no-TVS case, the ullage pressure immediately starts to increase since the liquid and vapor are already at an equilibrium temperature. The continuous operation of the TVS removes energy from the tank at a rate faster than it is being introduced from the environment, allowing a nearly constant pressure to be maintained in the tank. Even with the much higher heat input resulting from the loss of the insulation system, the TVS can remove sufficient heat to control the pressure in the tank. Under nominal heat input conditions the tank pressure would decrease with TVS operation.

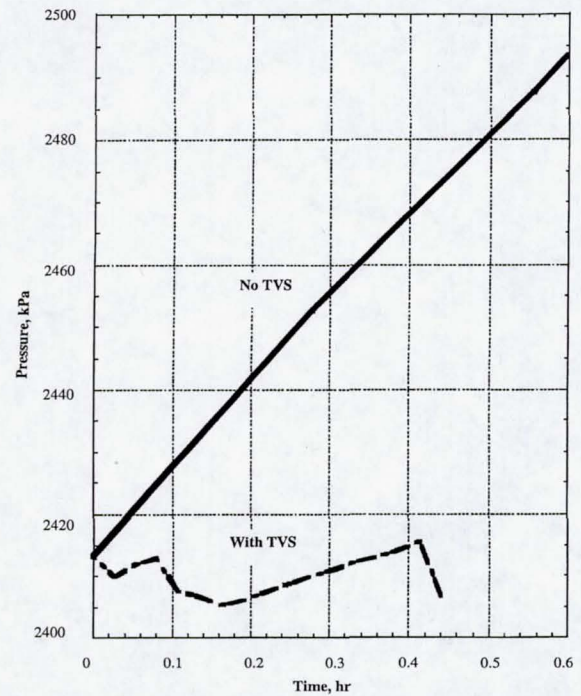


**Figure 7.** Ability of the thermodynamic vent system to handle the tank pressure following the loss of the insulation system.

### Conclusion

The use of ambient temperature helium to pressurize the OMS liquid oxygen tank was determined to be preferable to introducing the helium at the liquid oxygen temperature. The heat transfer from vapor to liquid will result in a temporary decrease in the tank pressure. The final tank pressure after 96 hrs will be significantly less than the case with cold helium. The higher helium temperature will also result in less mass of helium to pressurize the tank. No significant

thermal stratification was detected in the simulations performed. It was also found that a 5-minute period where the acceleration is increased from  $1 \times 10^{-5}$  g to  $1 \times 10^{-2}$  g in the opposite direction was insufficient to cause fluid mixing within the tank. With no fluid mixing there would be no pressure decrease even if a significant amount of thermal stratification were present.

#### Acknowledgement

We would like to extend thanks to Dr. Mohammad M. Hasan of the NASA Glenn Research Center for his assistance in this research effort.

#### References

- <sup>1</sup>E. Hurlbert, J. Applewhite, T. Nguyen, B. Reed, Z. Baojiong, W. Yue, "Non-Toxic Orbital maneuvering and reaction control systems for Reusable Spacecraft", *Journal of Propulsion and Power*, v14 n5, p 676-687, September-October 1998.
- <sup>2</sup>H. Rodriguez, "Non-Toxic System Architecture for Space Shuttle Applications", Boeing North American, Reusable Space Systems, 34<sup>th</sup> AIAA/ASME/SAE/ASEE, AIAA 98-3821, Cleveland, Ohio, July 13-15, 1998
- <sup>3</sup>W. Bailey and P. Uney, "System Evaluation of a Non-Toxic Upgrade for Shuttle OMS/RCS", Lockheed Martin Astronautics, AIAA 98-4034, Cleveland, Ohio, July 13-15, 1998
- <sup>4</sup>T. Lak, H. Rodriguez, F. Chandler, and D. Jenkins, "Non-Toxic Cryogenic Storage for OMS/RCS Shuttle Upgrade", AIAA 98-3818, Cleveland, Ohio, July 12-15, 1998
- <sup>5</sup>A. Hirata, K. Madoka, and O. Yasunori, 'Effect of Interfacial Velocity and Interfacial Tension Gradient on Momentum, Heat and Mass Transfer', *Canadian Journal of Chemical Engineering*, Volume 67, pp 777-786, October 1989
- <sup>6</sup>D. J. Lee, M. M. Telo da Gama, and K. E. Gubbins, 'Adsorption and Surface Tension Reduction at the Vapor-Liquid Interface', *Journal of Physical Chemistry*, No. 89, pp 1514-1519, 1985
- <sup>7</sup>J. O. Hirschfelder, C. F. Curtis, and R. B. Bird, "Molecular Theory of Gases and Liquids", Wiley, New York, 1954
- <sup>8</sup>G. R. Schmidt, A. Nadarajah, T. J. Chung, and G. R. Karr, 'Influence of Two-Phase Thermocapillary Flow on Liquid Retention in Microscopic Pores', *Journal of Thermophysics and Heat Transfer*, Vol. 9, No. 1, pp 151-158, January-March 1995
- <sup>9</sup>G. W. Burge, and J. B. Blackman, "Study and Design of Cryogenic Propellant Acquisition Systems - Vol. II," McDonnell Douglas Astronautics, MDC G5038, Huntington Beach, Ca, Dec. 1973
- <sup>10</sup>J. B. Blackman, "Design, Fabrication, Assembly and Test of a Liquid Hydrogen Acquisition Subsystem," McDonnell Douglas Astronautics, MDC G5360, Huntington Beach, Ca, May 1974
- <sup>11</sup>E. C. Cady, "Design and Evaluation of Thermodynamic Vent/Screen Baffle Cryogenic Storage System," McDonnell Douglas Astronautics, MDC G5360, Huntington Beach, Ca, June 1975
- <sup>12</sup>H. L. Paytner and G. R. Page, "Acquisition/Expulsion Orbital Propulsion System Study - Vol. II: Cryogenic Design," NASA CR-134154, Oct. 1973
- <sup>13</sup>R. P. Warren, "Acquisition System Environmental Effects Study," Martin Marietta, MCR-75-21, Denver, CO, May 1975
- <sup>14</sup>R. P. Warren, "Measurements of Capillary System Degradation," *AIAA Paper 75-1197*, Sept. 1975
- <sup>15</sup>F. O. Bennett, "Design and Demonstrate the Performance of Cryogenic Components Representative of Space Vehicles - Start Basket Liquid Acquisition Device Performance Analysis," General Dynamics, Space Systems Division, GDSS-CRAD-87-004, San Diego, Ca, Feb. 1987
- <sup>16</sup>J. S. Meserole and O. S. Jones, "Pressurant Effects on Cryogenic Liquid Acquisition Devices," *Journal of Spacecraft and Rockets*, Vol. 30, No. 2, p236-243, 1993
- <sup>17</sup>R. N. Herring and P. L. Barrick, "Gas-Liquid Equilibrium Solubilities for the Helium-Oxygen System", *International Advances in Cryogenic Engineering*, Vol. 10, pp 151-159, 1964
- <sup>18</sup>S. V. Patankar, Numerical Heat Transfer and Fluid Flow, Mc-Graw Hill, 1980
- <sup>19</sup>R.D. McCarty, "Interactive Fortran IV Computer Programs for the Thermodynamic and Transport Properties of Selected Cryogenes (Fluids Pack)", *NBS Technical Note 1025*, October 1980